Pergamon

Int. J. Solids Structures Vol. 33, No. 28, pp. 4239–4261, 1996

0020–7683/96 $15.00 + .00

0020–7683(95)00241–3

A TRANSFORMATION METHOD FOR IMPLEMENTING CLASSICAL MULTI-YIELD-SURFACE THEORY USING THE HARDENING RULE OF MROZ

DAR-YUN CHIANG
Institute of Aeronautics and Astronautics, National Cheng Kung University, Tainan, Taiwan 70101, R.O.C.

and

JAMES L. BECK
Division of Engineering and Applied Science, California Institute of Technology, Pasadena, California 91125, U.S.A.

(*Received* 9 *September* 1993; *in revised form* 3 *October* 1995)

Abstract—A new method for implementing classical multi-yield-surface theory using the kinematic hardening rule of Mroz is proposed, in which a response formula describing initial loading is introduced, and further unloading and reloading response is then found by applying a transformation to the stress state variables involved in the initial loading formula. The validity of the new formulation is supported by previous experimental results for biaxial cyclic nonproportional loading. The rules governing the response behavior under arbitrary loading paths also serve as a generalization of the Masing model for one-dimensional hysteresis and they provide instructive insight into material behavior in cyclic plasticity, such as the property of erasure of memory.

1. INTRODUCTION

1.1. *One-dimensional hysteretic models*

Numerous models have been proposed for one-dimensional nonlinear hysteretic response behavior of structural systems subject to arbitrary dynamic loading. These include the bilinear hysteretic model, the distributed-element model (Iwan, 1966), the Masing models (Jayakumar, 1987), the Bouc-Wen model (Wen, 1976, 1980), the Ozdemir model (1976), and so forth. The development of these hysteretic models has been primarily motivated by the desire to model the dynamic response of structures subjected to severe shaking from earthquakes. Of course, the earthquake response of real structures involves multi-axial cyclic plasticity. For this and other reasons, there has been much interest in developing constitutive models that can adequately predict multi-dimensional elastic-plastic response behavior of real materials and structures under arbitrary load paths.

Some researchers have attempted to extend the 1-D (one-dimensional) hysteretic models to the multi-dimensional case but this has proved to be a challenging task. For example, Park *et al.* (1986) proposed a 2-D (two-dimensional) hysteretic model for random vibrations of structures subject to biaxial excitations, which is an extension of the well-known 1-D non-deteriorating Bouc-Wen model (Wen, 1976). An important advantage of the 2-D Bouc-Wen model is that it is versatile and amenable to analytical treatment, and thus can be applied to systems of considerable complexity and under random excitation. However, the biaxial model inherits the disadvantage of the 1-D model which exhibits unstable drift under biased small cyclic excitations (Jayakumar, 1987), and so violates Drucker's postulates of stability (Sandler, 1978). In addition, there is another unrealistic

response feature inherent in the 2-D model, since under proportional (displacement) loading, the biaxial restoring force response is also proportional at all times, even if the response is in the plastic state. This behavior is not consistent with the theory of plasticity or experimental observations.

Recently, Graesser and Cozzarelli (1991) presented a systematic procedure for extending a 1-D model of hysteresis to a multi-dimensional tensorial representation provided that the model behavior is governed by simple power laws. In particular, they considered the generalization of the 1-D Ozdemir hysteretic model (Ozdemir, 1976). It can be easily shown, however, that this model is actually a special case of the Bouc-Wen model (Jayakumar, 1987), and hence it exhibits the same unstable behavior as mentioned earlier. As a result, the extended multi-dimensional model inherently exhibits unrealistic behavior, and again Drucker's postulates of stability are violated. The inconsistency of these generalized models (Bouc-Wen and Ozdemir models) with real behavior can be attributed partly to their simplified mathematical formulation and partly to lack of a physical basis.

Among the 1-D hysteretic models for structural dynamic analysis, the distributed-element model (DEM), introduced by Iwan (1966), can be thought of as physically motivated since it consists of an assemblage of simple ideal elasto-plastic elements. Recently, the DEM has been successfully extended to the multi-dimensional case so that it can be used for constitutive modeling of cyclic plasticity (Chiang and Beck, 1994a, b). While the formulation of the multi-dimensional DEM provides a useful and realistic way for analysis of general multi-axial cyclic response behavior, efficient numerical implementation of the theoretical formulation requires that only a limited number of elements be introduced, since the model response has to be found by keeping track of each element's behavior throughout the response history.

It has been shown (Jayakumar, 1987) that the 1-D DEMs actually fall within a general class of Masing models whose behavior is described by two simple rules which extend Masing's hypothesis (Masing, 1926) for steady-state hysteresis to arbitrary hysteretic behavior. The model response can therefore be found directly by employing these two rules without the need of tracing each element's behavior. An interesting question can then be raised: can we find mathematical rules similar to those previously used in the 1-D Masing models so that general multi-dimensional cyclic response can be found without keeping track of each element's behavior? If such mathematical rules do exist, then it may be possible to devise numerical schemes that are more efficient and more accurate than those based on tracking the behavior of a finite number of distributed elements.

We show in this paper that multi-dimensional plasticity under arbitrary loading can be modeled in an analogous way to Jayakumar's 1-D Masing models (1987). A response formula is introduced to describe initial loading, then further unloading and reloading responses are found by applying a transformation to the stress state variables involved in the initial loading formula. The response to arbitrary loading can then be described by two simple rules. Because of the choice of these rules, the model is equivalent to classical multi-yield-surface plasticity theory using the Mroz kinematic hardening rule.

1.2. *Multi-yield-surface plasticity and the Mroz hardening rule*

We give here a brief description of multi-yield-surface plasticity using the Mroz kinematic hardening rule (Mroz, 1967). In the formulation to be used, the yield surfaces are defined in stress space and they move around with the model response so that the current stress state of the model never lies outside any of the yield surfaces. The Mroz kinematic hardening rule specifies that the "active" yield surfaces on which the current stress state lies will translate in the same direction as the line joining the current stress point to that point on the next outermost yield surface which corresponds to the same direction of outward normal as that at the current stress point. This rule is sketched schematically in Fig. 1, where the point P is the current stress state on the active yield surface F_m and Q is the point on the outer surface F_{m+1} corresponding to the same direction of outward normal. The translation of the surface F_m (as well as the inner surfaces, such as F_{m-1}) will follow the direction given by the line PQ. The Mroz hardening rule ensures that the inscribed yield surfaces have a common tangent at the current stress point. In addition, it has been shown

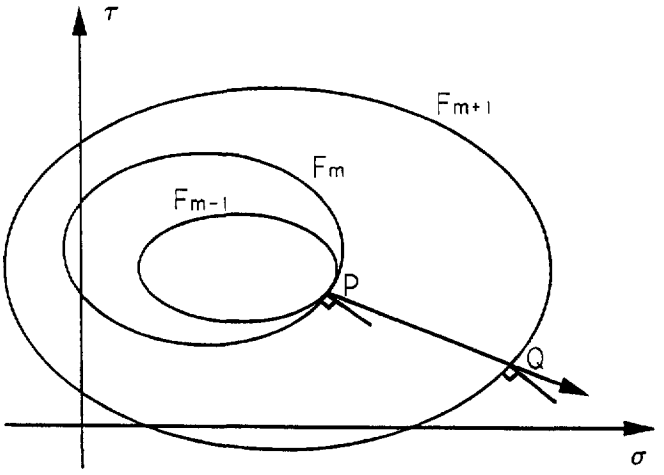

Fig. 1. The Mroz kinematic hardening rule.

mathematically that the rule never allows any two yield surfaces to intersect (McDowell, 1989).

It has been shown that a model based on the Mroz hardening rule can exhibit the observed response behavior of certain metals, such as equilibrium points and limit surface, while other often-used kinematic hardening rules for plasticity models, such as the Prager and Ziegler kinematic hardening rules, fail to exhibit such physical properties of response behavior (Lamba and Sidebottom, 1978). However, while the Mroz rule leads to good response predictions, its numerical implementation has been thought to be too involved and inefficient for complicated structural analysis because the positions of all the yield surfaces must be continuously tracked in the stress space (Lamba and Sidebottom, 1978; McDowell, 1989).

Krieg (1975) presented a two-surface approach which uses the concept of a loading surface and a limit surface. In Krieg's model, an analytical function is introduced to replace the field of several intermediate loading surfaces used by Mroz (1967) in his multi-yield-surface theory, so that the model can exhibit smooth transition from elastic to fully plastic state and its numerical implementation is more efficient.

Chu (1984, 1987) proposed an efficient model for implementing multi-yield-surface plasticity based on the Mroz hardening rule. In Chu's model, only the largest yield surface reached during every continuous loading or unloading path needs to be stored for response calculations, even though there is a field of continuously-distributed yield surfaces. The active yield surface, defined as the largest yield surface among those currently translating with the stress state, determines the instantaneous modulus for calculation of elastic-plastic response, while the modulus associated with each yield surface is obtained from an assumed universal stress-strain curve. Although Chu's model serves as an efficient way of implementing classical multi-yield-surface theory based on the Mroz hardening rule, the position of the active yield surface has to be updated in every loading or unloading step.

In the following, new response formulas based on classical multi-yield-surface theory with the Mroz hardening rule will be proposed which not only give a plasticity model which is computationally efficient and accurate but which also provide a generalization of the Masing models for one-dimensional hysteresis to multi-dimensional cyclic plasticity.

2. GENERALIZED MASING MODELS FOR MULTI-DIMENSIONAL PLASTICITY

Motivated by Masing's hypothesis for 1-D hysteresis (Masing, 1926), we propose new response formulas and rules for modeling of multi-dimensional plasticity. To make the

ideas clearer, we first introduce Masing's hypothesis and some extended rules that were proposed for modeling of 1-D hysteretic response behavior (Jayakumar, 1987).

2.1. *Masing's hypothesis and extended rules for one-dimensional hysteresis*

Masing (1926) asserted that if the force-displacement curve for a system at the initial loading is described by

$$f(r, x) = 0 \tag{1}$$

where r is the restoring force corresponding to the displacement x of the system, then the unloading and reloading branches of the steady-state hysteretic response of the system are geometrically similar to the initial loading curve except for a two-fold magnification, and are described by

$$f\left(\frac{r-r_0}{2}, \frac{x-x_0}{2}\right) = 0 \tag{2}$$

where (x_0, r_0) is the load reversal point for that particular loading branch. Note that the function f should satisfy

$$f(-r, -x) = f(r, x) \tag{3}$$

so that the initial force-deflection curve is symmetric about the origin. The above assertion is usually referred to as Masing's hypothesis for steady-state cyclic hysteretic response. A schematic diagram illustrating Masing's hypothesis is shown in Fig. 2.

The model behavior obtained using Masing's hypothesis is consistent with experimental observations of the Bauschinger effect occurring in some metals. Some properties of response behavior using Masing's hypothesis were summarized in Jayakumar (1987). One major concern associated with the original Masing's hypothesis is that it is useful only for steady-state cyclic response or loading between fixed limits. In the case of non-steady response, or loading between variable limits, where the response is not cycled around the same closed hysteresis loop, the hypothesis was considered to be of no help. However, Jayakumar (1987) proposed an extension of Masing's hypothesis by stipulating the following two general hysteresis rules so that simple and physical behavior for arbitrary hysteretic response can be obtained.

Rule 1 : *Incomplete loops.* The equation of any hysteretic response curve can be obtained by applying the original Masing rule to the virgin loading curve using the latest point of loading reversal.

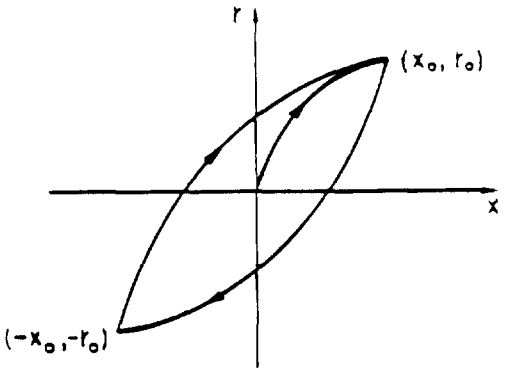

Fig. 2. Masing's hypothesis for cyclic hysteretic loops.

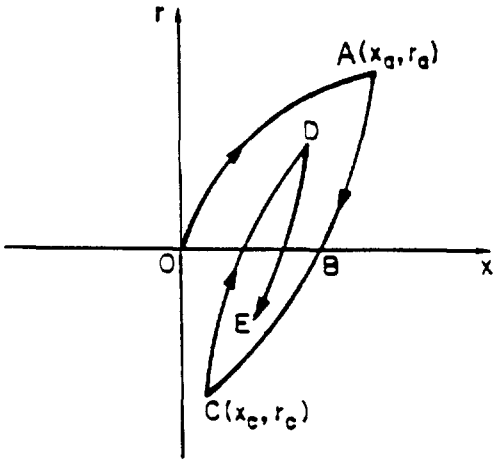

Fig. 3. Hysteretic loops for arbitrary response.

Consider, for example, the hysteretic loops shown in Fig. 3. If the virgin loading curve OA is characterized by eqn (1), then applying Rule 1, the equation for the branch curve CD will be

$$f\left(\frac{r-r_c}{2}, \frac{x-x_c}{2}\right)=0 \tag{4}$$

Based on this equation, it is easy to show that if the reloading curve CD in Fig. 3 had been continued, it would have formed a closed hysteresis loop given by $ABCDA$.

Rule 2 : *Completed loops*. The ultimate fate of an interior curve under continued loading or unloading is such that once it crosses a curve described in a previous load cycle, the force-deformation curve follows that of the previous cycle.

Based on Rules 1 and 2, if the unloading curve DE in Fig. 3 is continued, it will reach point C and then follow the extension of the curve ABC given by Rule 1.

An effective algorithm for numerical implementation of these extended Masing rules was proposed by Thyagarajan (1989), in which two load reversal points are removed from the memory list each time an interior response curve crosses a curve described in a previous load cycle. It has been shown (Jayakumar, 1987) that the hysteretic behavior of a distributed-element model (Iwan, 1966) can be completely described by these rules without the need of tracing each element's behavior. A special class of Masing models has been applied to system identification studies using inelastic pseudo-dynamic test data from a full-scale, six-story steel structure (Jayakumar and Beck, 1988).

2.2. *Response formula for initial loading*

To find mathematical rules similar to Masing's hypothesis for governing response behavior in multi-dimensional cyclic plasticity, one has to first introduce a formula describing the response to an initial loading, and then find corresponding rules describing subsequent response behavior. By initial loading here, we mean that no unloading defined according to the classical theory of plasticity has ever occurred. Recall that different loading cases for strain hardening materials are defined by introducing a *loading function* $F(\sigma_{ij})$, which is usually the same as the yield function, so that the cases of *loading*, *neutral loading*, or *unloading* correspond to

$$\mathrm{d}F=\frac{\partial F}{\partial \sigma_{ij}}\,\mathrm{d}\sigma_{ij}$$

being greater than, equal to, or less than zero, respectively.

A new response formula for initial loading is proposed here based on the response behavior of ideal plasticity and the introduction of a "modulus-reduction" function. We start with the relation between the plastic strain increment vector and the total strain increment vector in a yielding state of ideal plastic behavior:

$$d\boldsymbol{\varepsilon}^p = \begin{cases} \Lambda_0(\boldsymbol{\sigma})\, d\boldsymbol{\varepsilon} & \text{if } dF = 0 \\ 0 & \text{if } dF < 0 \end{cases} \tag{5}$$

where dF is a function of both the current state and the load increment, and the 6×6 matrix

$$\Lambda_0(\boldsymbol{\sigma}) = \frac{\mathbf{a}\mathbf{a}^T\mathbf{C}^e}{\mathbf{a}^T\mathbf{C}^e\mathbf{a}} \tag{6}$$

Here the 6×1 column vector $\mathbf{a}$ is the gradient of F with respect to the stress vector $\boldsymbol{\sigma}$, that is,

$$\mathbf{a} \equiv \nabla_{\sigma} F(\boldsymbol{\sigma}, \boldsymbol{\varepsilon}^p) \tag{7}$$

For ideal plasticity, dF is never greater than zero and $dF < 0$ corresponds to the case where the response is purely elastic. The assumed stress-strain relation is given in an incremental form by:

$$d\boldsymbol{\sigma} = \mathbf{C}^e\, d\boldsymbol{\varepsilon}^e = \mathbf{C}^e(d\boldsymbol{\varepsilon} - d\boldsymbol{\varepsilon}^p) \tag{8}$$

where $\mathbf{C}^e$ is the 6×6 elastic-modulus matrix. Thus, for model development, we need only focus on the generalization of the relation between $d\boldsymbol{\varepsilon}^p$ and $d\boldsymbol{\varepsilon}$.

For the purpose of developing a general response formula for initial loading, a *modulus-reduction* function which signifies the "degree of yielding" can be introduced as

$$D(\boldsymbol{\sigma}) = \left(\frac{F(\boldsymbol{\sigma})}{k_u}\right)^{n/2} \tag{9}$$

where $F(\boldsymbol{\sigma}) = k_u$ is the equation of the *limit surface* associated with the model and it can assume any appropriate form. $F(\boldsymbol{\sigma})$ also serves as the loading function controlling the cases of loading or unloading as defined above. The parameter n is introduced to control the smoothness of yielding, but the power law could be replaced by other functional forms. The response formula (5) for ideal plasticity and for initial loading is then modified by including the modulus-reduction function, so

$$d\boldsymbol{\varepsilon}^p = D(\boldsymbol{\sigma})\Lambda_0(\boldsymbol{\sigma})\, d\boldsymbol{\varepsilon} \tag{10}$$

The key point is that the modulus-reduction function $D(\boldsymbol{\sigma})$ replaces a conventional yield condition and subsequent hardening rules, so that continuous yielding behavior on initial loading is adequately modeled. Also, the model based on eqn (10) preserves all the equilibrium points and the limit surface of a perfectly plastic model (Chiang, 1992) so that it always leads to stable and physically consistent response behavior.

Consider the special case that $F(\boldsymbol{\sigma}) = 3J_2$, where $J_2 = \frac{1}{2}s_{mn}s_{mn}$ is the second invariant of the deviatoric stress tensor s_{ij}, that is, $F(\boldsymbol{\sigma})$ has the form of the von Mises yield function. When the response is small, $3J_2 \ll k_u$, and by eqns (9) and (10), we have $d\boldsymbol{\varepsilon}^p \approx 0$; when $3J_2 = k_u$, the response state reaches the limit surface associated with the model and the response behavior becomes perfectly plastic as loading is continued, since then $D(\boldsymbol{\sigma}) = 1$ in eqn (10).

A special case used later in the applications is biaxial tension-torsion involving axial stress and strain, σ and ε, and shear stress and strain, τ and γ. Equation (10) gives in this case:

$$\begin{aligned} d\varepsilon^p &= C\sigma[E\sigma\, d\varepsilon + \alpha G\tau\, d\gamma] \\ d\gamma^p &= \alpha C\tau[E\sigma\, d\varepsilon + \alpha G\tau\, d\gamma] \\ C &= \frac{D(\sigma,\tau)}{E\sigma^2 + \alpha^2 G\tau^2} \end{aligned} \tag{11}$$

where $D(\sigma,\tau) = [(\sigma^2+\alpha\tau^2)/\sigma_u^2]^{n/2}$ and where $\alpha = 3$ or 4 for the von Mises or Tresca yield function respectively, and σ_u is the ultimate (limit) uni-axial stress.

2.3. *Response formulas for unloading and reloading*

With the initial loading formula defined in eqn (10), we now want to find appropriate mathematical rules to govern unloading and reloading response behavior, so that the complete response history to any multi-dimensional loading path can be calculated. Unloading and reloading correspond to $dF < 0$ and $dF \geqslant 0$ respectively, where F is the same function as employed in eqn (9).

Masing's hypothesis for 1-D hysteresis implies mathematically that the behavior of the unloading and reloading response can be found from that of the virgin (initial loading) response by introducing a proper transformation of the state variables describing the response. Motivated by this concept and the behavior of a classical multi-yield-surface model using the Mroz kinematic hardening rule (Fig. 1), we propose the introduction of a transformation of the state variables involved in the initial loading formula (10), so that unloading and reloading response can be found from:

$$d\boldsymbol{\varepsilon}^p = D(\boldsymbol{\sigma}')\Lambda_0(\boldsymbol{\sigma}')\, d\boldsymbol{\varepsilon} \tag{12}$$

where $\boldsymbol{\sigma}'$ denotes the vector of the transformed stress state, which is a function of not only the current response state, but also the past history.

To determine the effective transformation required for our purpose, we remark that for the classical multi-yield-surface model, the yield surfaces reached by the current stress state must be carried along with the response state in such a way that they all have the current stress point as a common tangent point. The movement of the yield surfaces along with the current state is illustrated schematically in Fig. 4, where the circles represent yield "surfaces" in a 2-D stress space and points A, B denote two instantaneous stress states. Thus, the response behavior corresponding to the unloading branch from a point B can be found by transforming the geometrical configuration in Fig. 4(c) back into that in 4(a), so that eqn (12) can be used effectively for response calculation of any unloading (or reloading) branches. Care must be taken in performing the transformations so that not only the transformation of geometrical configurations is appropriately done, but also the normality rule for determining increments of plastic strain is preserved (see Appendix).

In the following, we will be concerned only with the 2-D loading case so that we need only deal with transformations of planar configurations. An effective transformation formula for "steady-state" cyclic response (i.e., loading between points on the same yield surface centered at the origin) that is derived from a composition of proper complex-valued transformations can be found as follows:

$$\sigma' + i\sqrt{\alpha}\tau' = \frac{r_1}{2\sin\theta_2} e^{-i\theta_4} \tag{13}$$

where (σ', τ') denotes the transformed stress state, $\alpha = 3$ or 4 for the von Mises or Tresca yield function, respectively, and

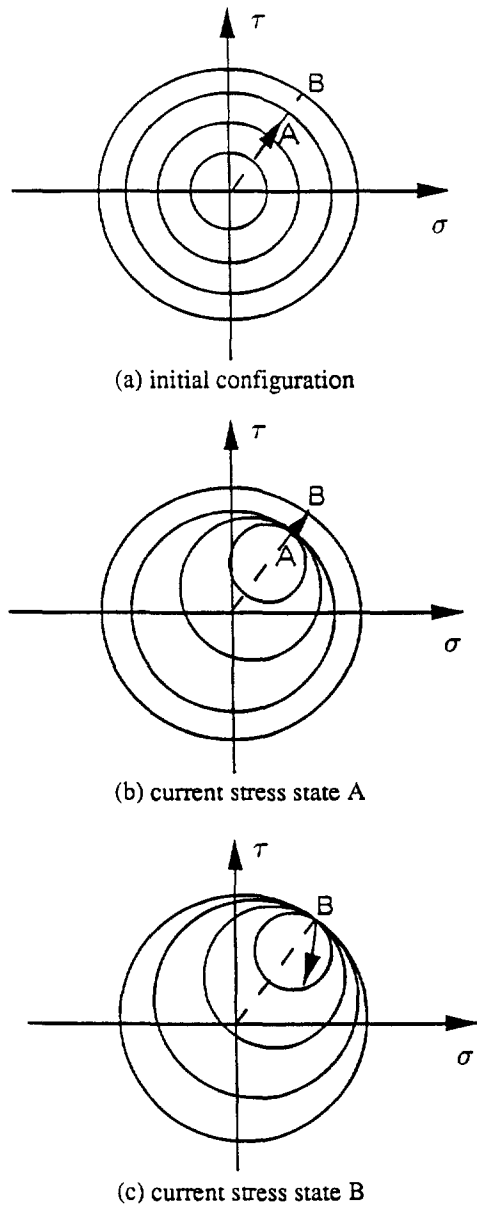

Fig. 4. Movement of yield surfaces with current stress state moving from A to B; (a) initial configuration; (b) current stress state A; (c) current stress state B.

$$r_1 = \sqrt{(\sigma-\sigma_0)^2+\alpha(\tau-\tau_0)^2}$$

$$\theta_1 = \tan^{-1}\left(\frac{\sqrt{\alpha}(\tau-\tau_0)}{\sigma-\sigma_0}\right), \quad \theta_0 = \tan^{-1}\left(\frac{\sqrt{\alpha}\tau_0}{\sigma_0}\right)$$

$$\theta_2 = \theta_1-\theta_0+\frac{\pi}{2}, \quad \theta_4 = \pi-2\theta_1+\theta_0 \tag{14}$$

where the principal values are used for the inverse tangents, (σ, τ) is the current stress state and (σ_0, τ_0) is the stress state corresponding to the last point of load reversal. The detailed derivation of the transformation (13),(14) is given in the Appendix where it is explained how any 2-D yield function can be treated. A simple geometric interpretation for the transformation is that eqn (13) gives the σ and τ components of the stress vector of the

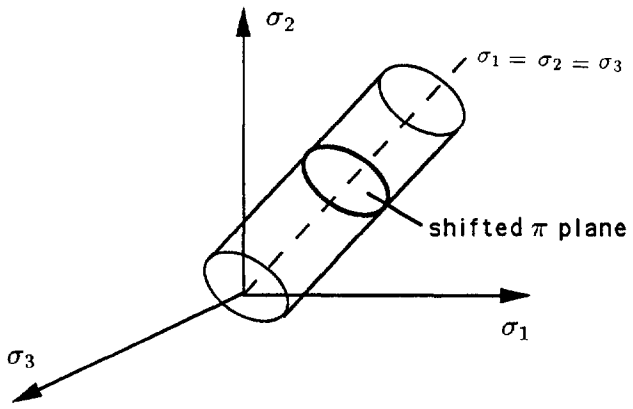

(a) von Mises yield condition

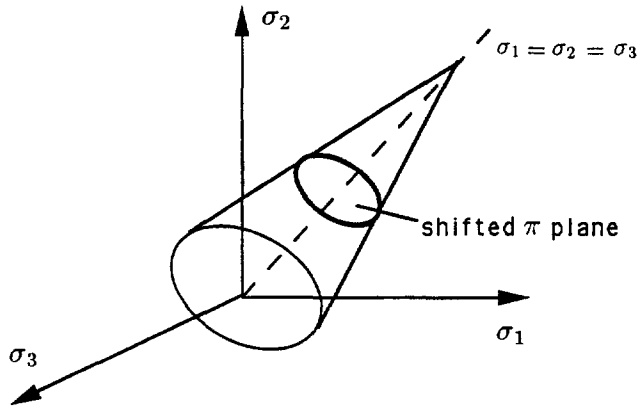

(b) Drucker-Prager yield condition

Fig. 5. Different yield surfaces and shifted π-planes in the principal stress space; (a) von Mises yield condition; (b) Drucker-Prager yield condition.

current stress state relative to the center of the active yield surface on which the stress state lies.

The transformation approach given above is only for the 2-D case. However, it is also applicable to general multi-dimensional plasticity provided that isotropic materials are considered and the plastic deformation can be treated as independent, or as some simple function, of the hydrostatic stress state. Many real materials exhibit approximately these kinds of behavior, such as metals and soils. In this case, we can always convert a stress state (which is a symmetric two-tensor) into a corresponding principal stress state (a diagonal two-tensor) for which the shear stress components vanish, and apply the 2-D transformations to the stress state projected on a shifted π-plane which is perpendicular to the hydrostatic axis $\sigma_1 = \sigma_2 = \sigma_3$ in the principal stress space. This is shown in Fig. 5(a) and 5(b), in which the circular cylinder and cone represent the yield surfaces corresponding to the von Mises and Drucker-Prager yield conditions (Bathe, 1982), respectively. A schematic diagram illustrating this idea of transformation on the π-plane is shown in Fig. 6.

2.4. *Response rules for arbitrary loading histories*

With the initial response formula (10) and the transformation (12)–(14) for unloading and reloading, we are able to determine the steady-state cyclic response of a system characterized by multiple yield surfaces without the need to calculate the response of

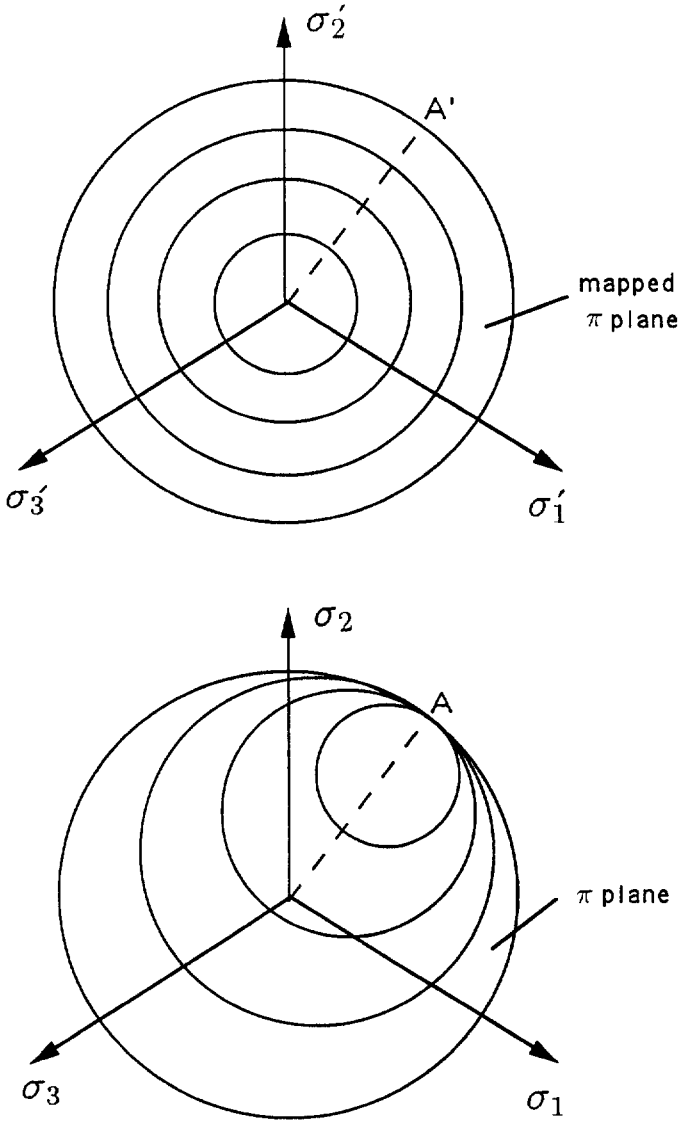

Fig. 6. Transformation on the π-plane when A' is the image of A.

elements or to trace the motions of yield surfaces. In the general cyclic loading case, we still need to extend the foregoing formulae, as Jayakumar (1987) did for 1-D hysteresis by extending Masing's hypothesis.

In the 1-D case, the response rules were proposed for incomplete and completed hysteresis loops. In the multi-dimensional case, however, the cyclic loops between fixed strain points may not be "strictly closed" in general. Here, by "strictly closed" we mean that a stress-strain loop is closed at a load reversal point so that this point is both the starting and the ending point of the loop. Based on geometrical considerations of multiple yield surfaces and the Mroz hardening rule, we can modify the definitions for incomplete and completed loops and deduce corresponding rules for them in the general multi-dimensional case.

First, we define a *half loop* as the path between two consecutive load reversals and a *loop* as two consecutive half loops. We can then define a *completed loop* as a loop along which the outermost yield surface that contains the last two points of load reversal is reached again during the loading process. Otherwise, the loop is said to be *incomplete*. For example, in Fig. 7, the stress response loop ABC is incomplete, while the loop BCE is a completed one since the outermost yield surface (labelled 2) containing the last two points

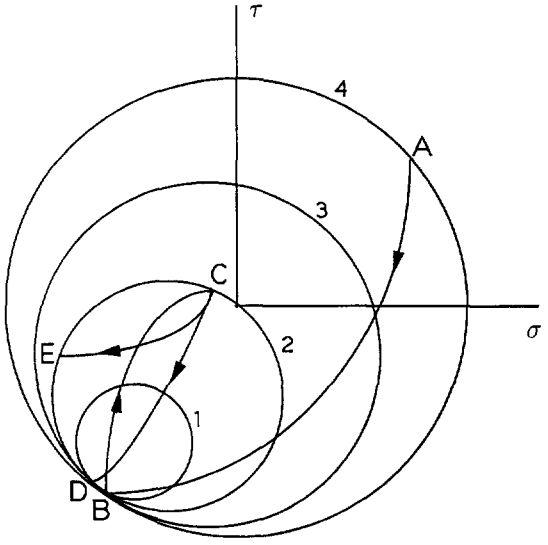

Fig. 7. Illustration of completed loops and numerical difficulty associated with the transformation approach.

of load reversal B and C is reached at E. With these definitions we can propose the following two rules for arbitrary response.

Rule 1 : *Incomplete loops.* The equation of any response curve can be obtained simply by using eqn (12) and applying the $\boldsymbol{\sigma}-\boldsymbol{\sigma}'$ transformation, as given by eqns (13) and (14), to the last point of load reversal (σ_0, τ_0) and the outermost yield surface on which (σ_0, τ_0) lies. (The dependence on the outermost yield surface is described below.)

For example, the response curve CE in Fig. 7 can be found by applying the transformation rule to point C and yield surface 2.

Rule 2: *Completed loops.* Once the stress state reaches the outermost yield surface on which the last two load reversals occurred, the transformation rule is switched from the last point of load reversal to the previous one, along with its corresponding outermost yield surface.

For example, in Fig. 7, as the loop BCE is completed at E, the transformation rule is then applied to point B and yield surface 4 for the response that follows. Note that Rule 2 for completed loops is different from that in the 1-D case where two points of load reversal are erased at a time when an interior curve crosses a curve from a previous load cycle. This rule for 1-D hysteresis can actually be shown to be a special case of the 2-D rule when only proportional loading occurs.

We remark that, in the case of arbitrary response, the geometrical configuration of yield surfaces is different from that of a steady-state case, not only in the position of the active point of load reversal, but also in that θ_0 in (14) is measured by reference to a new center point, which may be different from the origin of the stress space. Therefore, the equation for θ_0 in (14) should be replaced by the more general formula

$$\theta_0 = \tan^{-1}\left(\frac{\sqrt{\alpha}(\tau_0-\tau_C)}{\sigma_0-\sigma_C}\right) \tag{15}$$

where (σ_C, τ_C) represents the coordinates of the center of the current reference circle (the outermost yield surface that the last load reversal point is on) and (σ_0, τ_0) is the stress state

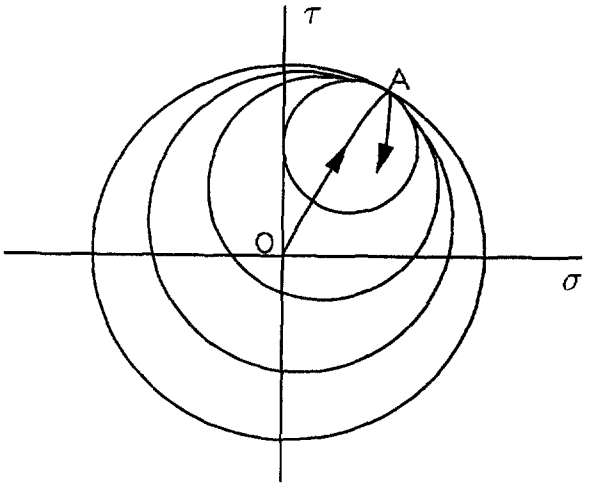

(a) unloading from point A

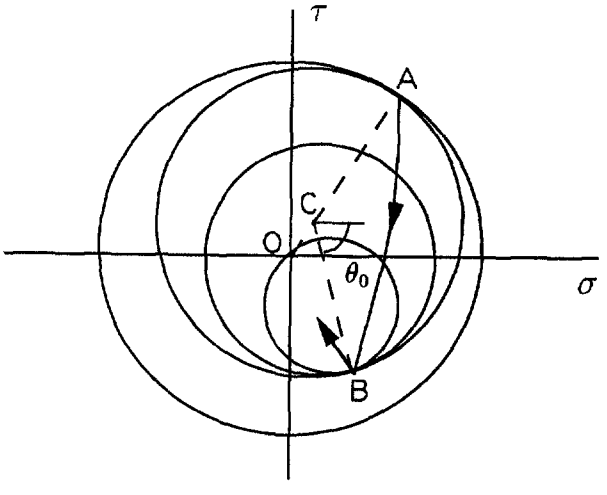

(b) unloading from point B with new center C

Fig. 8. Geometrical consideration of arbitrary response; (a) unloading from point A; (b) unloading from point B with new center C.

corresponding to the last load reversal point. This situation is illustrated in Fig. 8. Figure 8(a) shows the process of *initial* loading from the origin O to point A and then unloading from there. In this case, upon unloading from point A, the current reference circle is centered at the origin of the stress space. Figure 8(b) shows the geometrical configuration corresponding to unloading from point B, where θ_0 is given by (15) with $(\sigma_0, \tau_0) = (\sigma_B, \tau_B)$ and where point C represents the center of the current reference circle. The coordinates of the new center point C are given by

$$(\sigma_C, \tau_C) = (\sigma_A, \tau_A) - \frac{r_B}{r_A}(\sigma_A - \sigma_{C'}, \tau_A - \tau_{C'}) \tag{16}$$

where r_A and r_B denote the radii of the outermost "active" circles on which points A and B lie respectively, and $(\sigma_{C'}, \tau_{C'})$ represents the coordinates of the center of the previous reference circle. (C' coincides with the origin O for the case in Fig. 8.)

Based on the preceding rules, numerical implementation of the foregoing algorithm requires that for each point of load reversal, the yield constant (radius) and the coordinates of the center point of the outermost yield surface on which the reversal point lies both be

stored in a list. Every time the yield surface with the smallest yield constant in the memory list is again reached, its corresponding point of load reversal and center of reference is erased from the memory.

While the mathematical manipulation involved in the above approach based on transformation formulas is simple and effective, a major problem of implementing the above rules for arbitrary response exists. This problem is associated with the numerical ill-conditioning which occurs when the response formulae are applied to states near the points of load reversal, which are singular points of the corresponding transformations employed, as can be deduced from the derivation of the transformation formulas. To illustrate this, we consider the following example. When unloading occurs from a point, say the point B or C in Fig. 7, the loading function, $F(\boldsymbol{\sigma}')$, at any point on curve BC or CE is computed by reference to the corresponding unloading point B or C. After a loop is completed, such as the loop BCD or BCE in Fig. 7, the loading function value at D or E should be calculated by reference to the previous unloading point B, according to the Rule 2 stated above. However, when the point at which a loop is completed is very close to the previous unloading point (such as point D in Fig. 7 which is close to point B), due to the singular behavior of the transformation at a load reversal point, the loading function value cannot be found accurately. In other words, the calculation of $\boldsymbol{\sigma}'$ from the transformation formulas is numerically ill-conditioned.

A remedy for dealing with this problem is that the two latest points of load reversal, instead of just one (Rule 2), will be erased every time a loop is completed if the current loading function value with reference to the previous point of load reversal is found to be considerably less than the yield constant of the active yield surface on which the latest point of load reversal lies. For example, in Fig. 7, the points D and E, which both lie on yield surface 2, should have the same loading function value, say F_2. But due to the singular behavior around the load reversal point B, the loading function value at D may be found numerically to be much less than F_2, e.g., if point D coincides with (or is very close to) the load reversal point B, the loading function value will be found to be zero there. In this case, we may erase two latest points of load reversal, i.e., B and C in Fig. 7, so that the active load reversal point becomes A and then the loading function value at D with reference to A will be found to be about F_4 (corresponding to yield surface 4), which is correct for continued response from D. On the other hand, if the response curve goes from C to E at which the loading function value with reference to point B is close to the loading function value F_2 of the active yield surface 2, then only one point of load reversal (point C) will be removed from the memory.

The above rules for the sub-cycling type of behavior have features which are similar to those proposed by Chu (1984). However, with the transformation technique introduced above, there is no need to keep track of the movement of the active yield surface in every loading step. Instead, only the position of the active yield surface corresponding to each load reversal state is required. This feature that the current reference yield surface in the proposed model is unchanged between two consecutive load reversal states alleviates the problem of error accumulation that might be experienced in the numerical implementation of Chu's model.

3. SIMULATION STUDIES

Based on the classical formulation of ideal plasticity and multi-yield-surface theory, we have derived a class of "generalized Masing models" for multi-dimensional cyclic loading based on the response formula (10) for initial loading, together with the transformation formulae (12)–(14), and the two rules governing the rest of a response history. It is of interest to examine the performance of such a model that is actually composed of an infinite number of yield surfaces moving in the stress space according to the Mroz kinematic hardening rule. In the following, the model performance will be evaluated under some biaxial tension-torsion loading conditions for which experimental results are available for comparison from the literature.

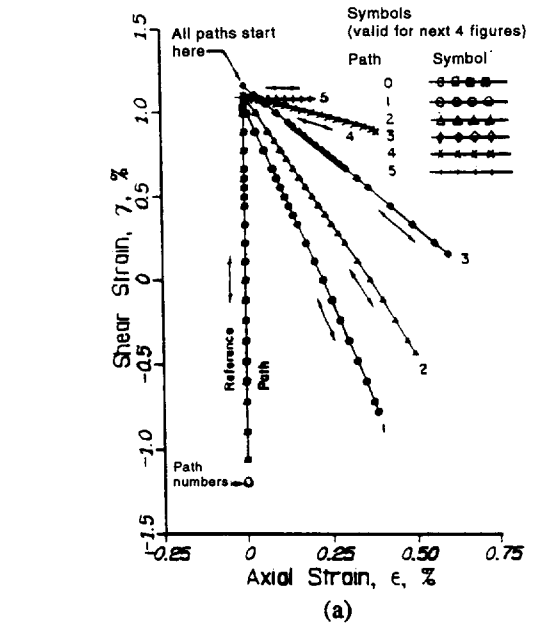

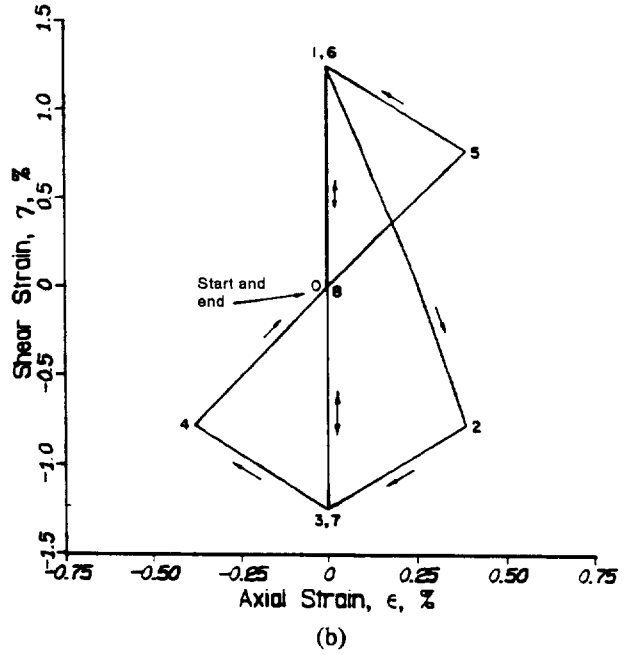

Fig. 9. Prescribed strain loading paths for response studies of the proposed generalized Masing model (from Lamba and Sidebottom, 1978).

Lamba and Sidebottom (1978a, b) conducted a series of biaxial tension-torsion tests on thin-walled copper tubes in which cyclic, nonproportional axial-torsional strain paths were applied to examine material response behavior after the material had been cyclically stabilized. Two of the prescribed strain loading paths are shown in Fig. 9, and the corresponding experimentally-observed stress responses are shown in Figs 10 and 11. Note that the loading path sequence in Fig. 9(a) is 0-1-0-2-0-3-0-..., so as to study the property of "erasure-of-memory" (Lamba and Sidebottom, 1978a; Chiang, 1992; Chiang and Beck, 1994a, b). Also, the stress path resulting from the repetition of path 0 each time is not plotted in Fig. 10(a) for clarity.

The results of response predictions using a generalized Masing model for the prescribed strain paths are shown in Figs 12 and 13, where both Tresca's and von Mises' yield criteria

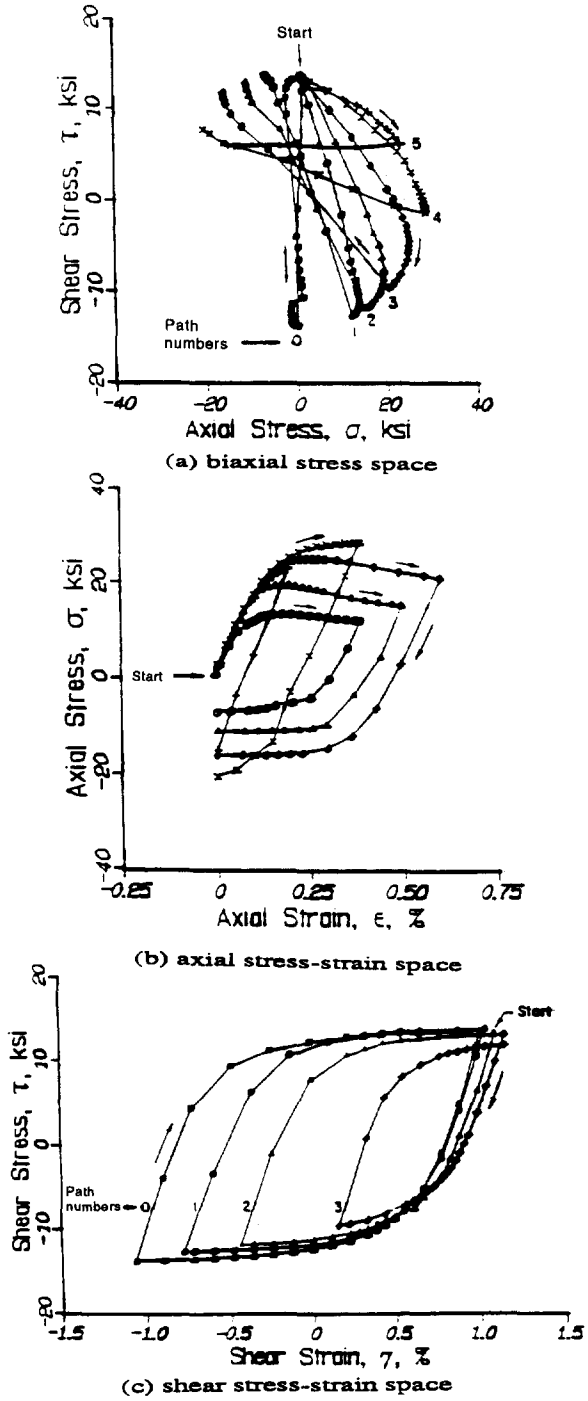

Fig. 10. Experimentally-observed stress response of copper to the prescribed strain path given in Fig. 9(a) (from Lamba and Sidebottom, 1978).

have been used in the modulus-reduction function as in eqn (11). In the simulations, the model parameters used were $E = 16{,}700$ ksi, $\nu = 0.33$, $\sigma_u = 30$ ksi, and $n = 2.5$. The experimental results and simulations are for cyclically stabilized behavior, so the parameter k_u ($=\sigma_u^2$ here) in the modulus-reduction function of eqn (9) is taken as a constant. The model could be extended to cyclically hardening or softening processes by taking k_u as an appropriate experimentally-determined function of the plastic work or the accumulated plastic deformation.

A comparison between the model predictions and the experimentally-observed results (Figs 10 and 12, and Figs 11 and 13), leads to the following remarks. It is immediately

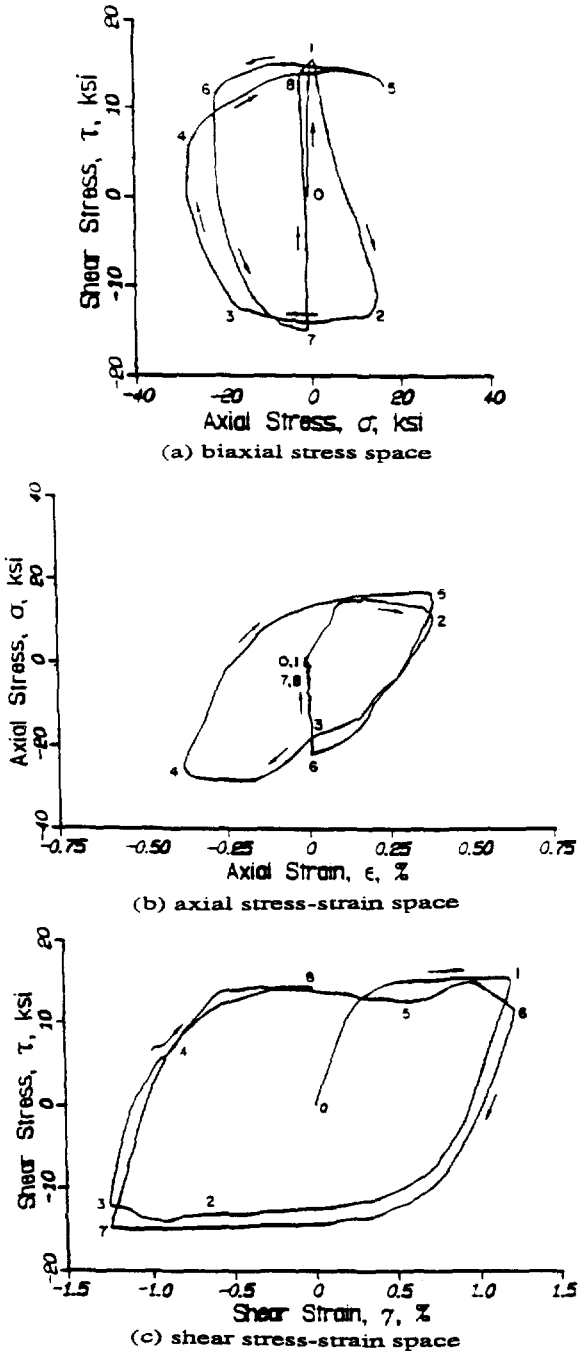

Fig. 11. Experimentally-observed stress response of copper to the prescribed strain path given in Fig. 9(b) (from Lamba and Sidebottom, 1978).

recognized that the response behavior described by the initial loading formula (11) and the transformation rules 1 and 2 is in good agreement with the experimental results in almost every aspect. Tresca's yield condition leads to a slightly better result than von Mises' yield condition for the value of the ultimate shear stress predicted, but for both yield conditions, transition from the elastic regime to the plastic regime is smooth and well-behaved, and the complicated biaxial Bauschinger effect is also well accounted for. Moreover, the model behavior clearly shows the existence of equilibrium points and a limit surface, as well as the property of erasure of memory (e.g., in Fig. 12, every time strain path 0 in Fig. 9(a) is followed, the model always ends up with the same stress state regardless of what the previous history was). A comparison of the predictions of Chu's model with the experimental results

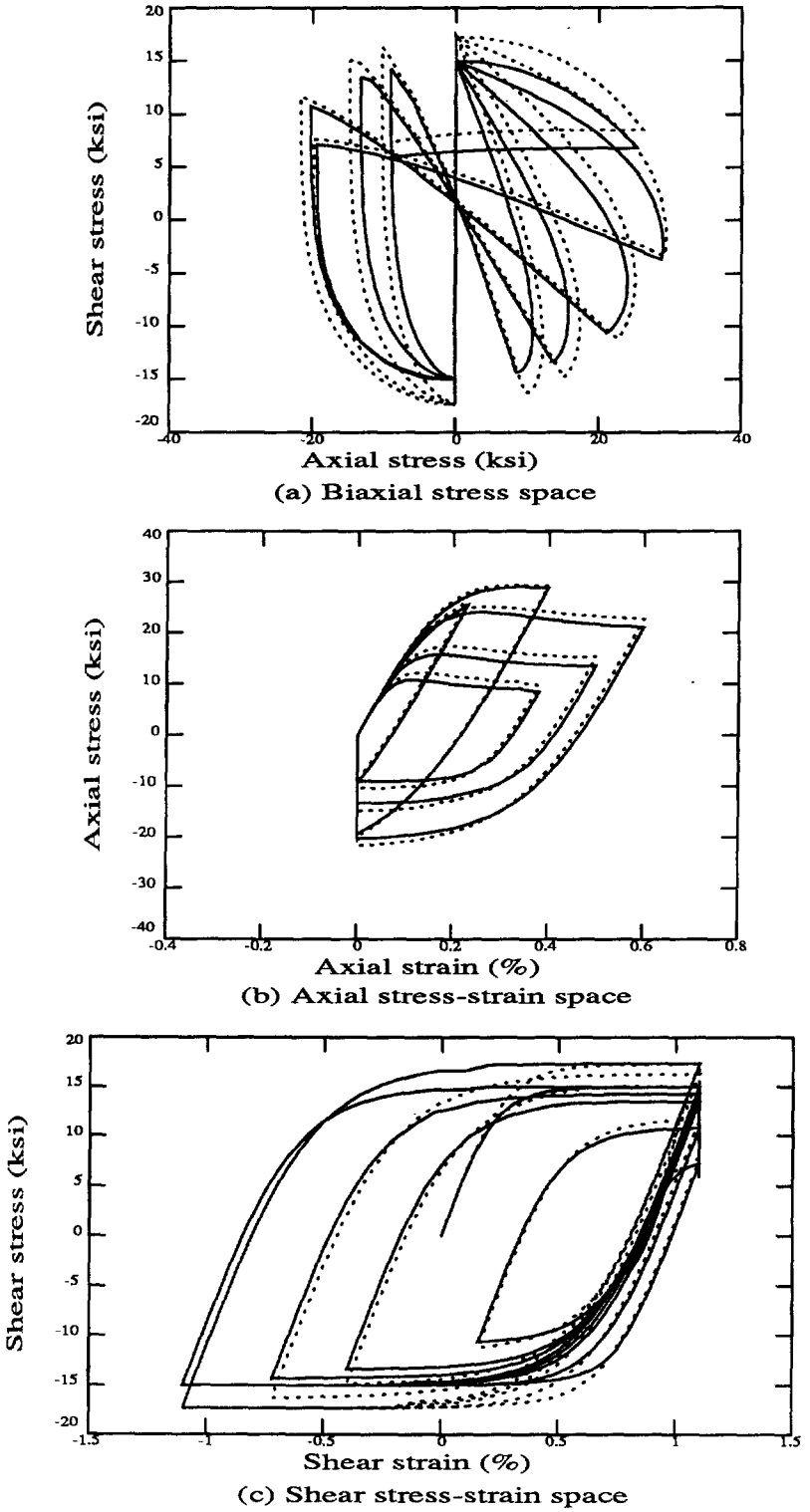

Fig. 12. Stress response predicted by a generalized Masing model subject to the prescribed strain path given in Fig. 9(a) (Tresca ——, von Mises – – –).

for the same strain loading path as shown in Fig. 9(a), shows that these latter features are not exhibited by her model (Chu, 1987).

The physical consistency and excellent accuracy of the model in response prediction may be attributed to the adequate response formulas which utilize the concept of a limit surface, an uncountably infinite number of yield surfaces and the well-formulated Mroz

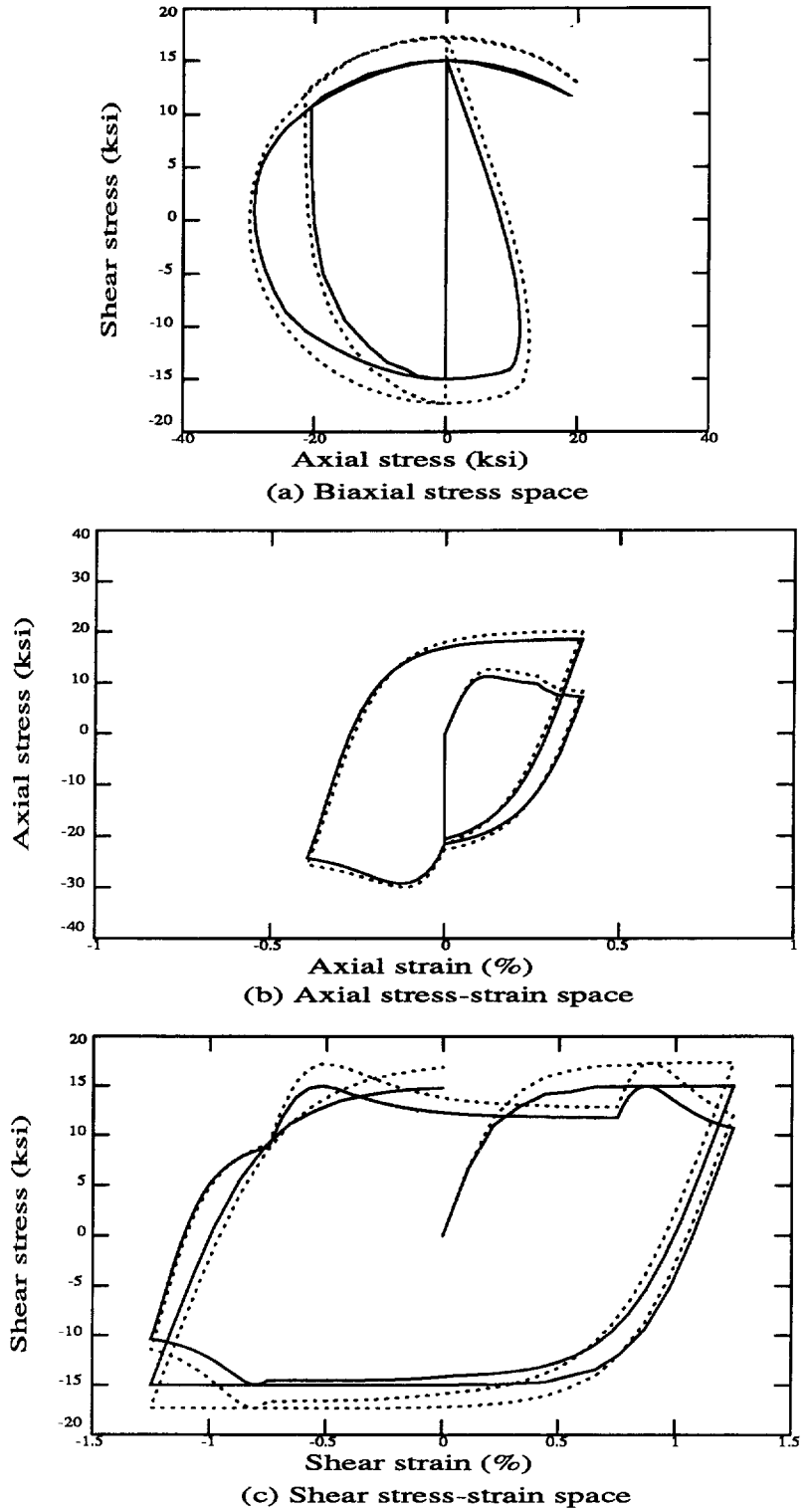

Fig. 13. Stress response predicted by a generalized Masing model subject to the prescribed strain path given in Fig. 9(b) (Tresca ——, von Mises – – –).

kinematic hardening rules. In addition, the computational effort in making response predictions based on the above response-formula approach is very low. The numerical efficiency of the model is due to the proposed transformation method which avoids the costly bookkeeping involved in moving multiple yield surfaces around in the stress space.

4. CONCLUSION

A class of generalized Masing models for cyclic plasticity is proposed based on a plane-geometry transformation method. A response formula valid for initial loading is introduced by considering the behavior of ideal plasticity and introducing a modulus reduction function which utilizes the concept of a limit surface. The proposed transformation method, when combined with appropriate response rules proposed for different loading branches, not only gives good predictions of the biaxial behavior of thin-walled copper tubes but also gives better insight into material behavior in cyclic plasticity, such as the property of erasure of memory. Furthermore, this new method provides an efficient way of implementing classical multi-yield-surface theory with the kinematic hardening rules of Mroz, as well as providing a unified concept for generalizing 1-D hysteresis to multi-dimensional plasticity.

Acknowledgement—The authors wish to thank an anonymous reviewer for pointing out the earlier work done by C.-C. Chu.

REFERENCES

Bathe, K. J. (1982). *Finite Element Procedures in Engineering Analysis*, Prentice-Hall, New Jersey.
Chiang, D. Y. (1992). Parsimonious modeling of inelastic systems. Report No. EERL 92-02, California Institute of Technology, Pasadena.
Chiang, D. Y. and Beck, J. L. (1994a). A new class of distributed-element models for cyclic plasticity—part 1: theory and application. *Int. J. Solids Structures* **31,** 469–484.
Chiang, D. Y. and Beck, J. L. (1994b). A new class of distributed-element models for cyclic plasticity—part 2: on important properties of material behavior. *Int. J. Solids Structures* **31,** 485–496.
Chu, C.-C. (1984). A three-dimensional model of anisotropic hardening in metals and its application to the analysis of sheet metal formability. *J. Mech. Phys. Solids* **32,** 197–212.
Chu, C.-C. (1987). The analysis of multiaxial cyclic problems with an anisotropic hardening model. *Int. J. Solids Structures* **23,** 569–579.
Graesser, E. J. and Cozzarelli, F. A. (1991). A multi-dimensional hysteretic model for plastically deforming metals in energy absorbing devices. Report No. NCEER 91-06, State University of New York, Buffalo.
Iwan, W. D. (1966). A distributed element model for hysteresis and its steady-state dynamic response. *J. Appl. Mech., ASME* **33,** 893–900.
Jayakumar, P. (1987). Modeling and identification in structural dynamics. Report No. EERL 87-01, California Institute of Technology, Pasadena.
Jayakumar, P. and Beck, J. L. (1988). System identification using nonlinear structural models. In *Structural Safety Evaluation Based on System Identification Approaches* (eds H. G. Natke and J. T. P. Yao), pp. 82–102, Vieweg-Verlag, Wiesbaden.
Krieg, R. D. (1975). A practical two surface plasticity theory. *J. Appl. Mech., ASME* **42,** 641–646.
Lamba, H. S. and Sidebottom, O. M. (1978a). Cyclic plasticity for nonproportional paths—part 1: cyclic hardening, erasure of memory, and subsequent strain hardening experiments. *J. Engng Mat. Tech.* **100,** 96–103.
Lamba, H. S. and Sidebottom, O. M. (1978b). Cyclic plasticity for nonproportional paths—part 2: comparison with predictions of three incremental plasticity models. *J. Engng Mat. Tech.* **100,** 104–111.
Masing, G. (1926). Eigenspannungen und verfestigung beim messing (Self stretching and hardening for brass). In *Proc. 2nd International Congress for Applied Mechanics*, Zurich, Switzerland, pp. 332–335 (in German).
McDowell, D. L. (1989). Evaluation of intersection conditions for two-surface plasticity theory. *Int. J. Plasticity* **5,** 29–50.
Mendelson, A. (1968). *Plasticity: Theory and Application*, Macmillan, New York.
Mroz, Z. (1967). On the description of anisotropic workhardening. *J. Mech. Phys. Solids* **15,** 163–175.
Ozdemir, H. (1976). Nonlinear transient dynamic analysis of yielding structures. Ph.D. dissertation, Department of Civil Engineering, University of California, Berkeley.
Park, Y. J., Wen, Y. K. and Ang, A. H-S. (1986). Random vibration of hysteretic systems under bi-directional ground motions. *Int. J. Earthquake Engng Struct. Dyn.* **14,** 543–557.
Sandler, I. S. (1978). On the uniqueness and stability of endochronic theories of material behavior. *J. Appl. Mech., ASME* **45,** 263–266.
Spiegel, M. R. (1964). *Theory and Problems of Complex Variables*, Schaum's Outline Series in Mathematics, McGraw-Hill.
Thyagarajan, R. S. (1989). Modeling and analysis of hysteretic structural behavior. Report No. EERL 89-03, California Institute of Technology, Pasadena.
Wen, Y. K. (1976). Method for random vibration of hysteretic systems. *J. Engng Mech., ASCE* **102,** 249–263.

APPENDIX: DERIVATION OF TRANSFORMATION FORMULAE

In the following, we derive the transformation in eqns (13) and (14) using classical multi-yield-surface theory based on the Mroz kinematic hardening rule. In the derivation, we assume that the yield surfaces in the 2-D σ–τ stress space can be represented by circles which are initially concentric. This, however, need not put any limitation on applications, since according to the well-known Riemann Mapping Theorem, a simply-connected region of arbitrary shape can always be mapped onto a circular region through a mapping conformal on its interior. The

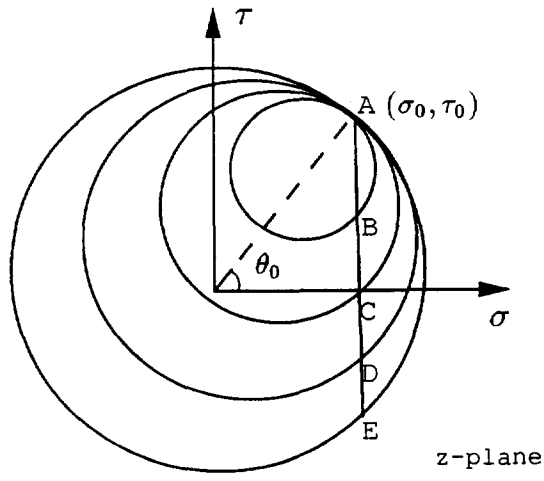

(a) configuration before transformation

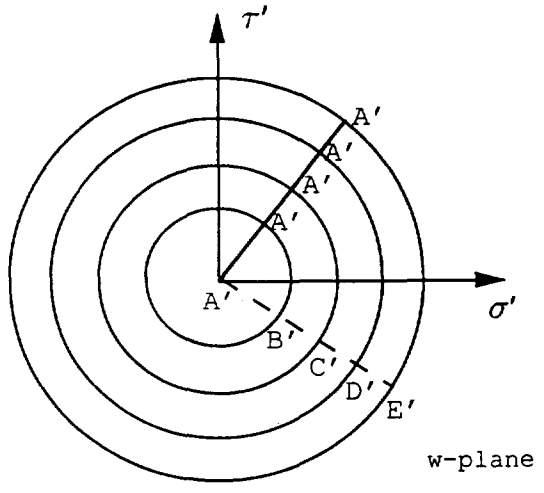

(b) configuration after transformation

Fig. A.1. Geometrical configurations before and after transformation.

same theorem has also been extended to the case where a region bounded by two simple closed curves, one inside the other, is mapped into a region bounded by two concentric circles (Spiegel, 1964). Therefore, the yield surfaces in the 2-D space can be of any shape and the derived transformation can still be employed, as long as a conformal mapping can be found so that the yield surfaces can be transformed into circles.

In order to employ the same response formula (e.g., eqn (10)) for all response branches in the multi-dimensional case, the stress state variables $\boldsymbol{\sigma}$ involved in the response formula should be modified by a suitable transformation, as suggested by Masing's hypothesis for cyclic hysteretic response in the 1-D case. The transformation must be able to characterize the different response branches so as to appropriately reflect the behavior corresponding to different loading conditions.

Consider the two response situations in Fig. A.1(a) and (b), in which the multi-dimensional yielding behavior is accounted for by classical multi-yield-surface theory with the Mroz kinematic hardening rule. The idea proposed here is that if we can find a transformation formula that maps the geometrical configuration in Fig. A.1(a) to that in A.1(b), then we can use the initial-loading response formula to describe the response corresponding to subsequent unloading or reloading branches. To transform the geometrical configuration in Fig. A.1(a) to that in Fig. A.1(b), we introduce a series of complex-valued mappings as follows:

$$w_1 = z-(\sigma_0+i\tau_0): \quad (w_1 \equiv \sigma_1+i\tau_1 \equiv r_1 e^{i\theta_1}, \quad z \equiv \sigma+i\tau) \tag{I}$$

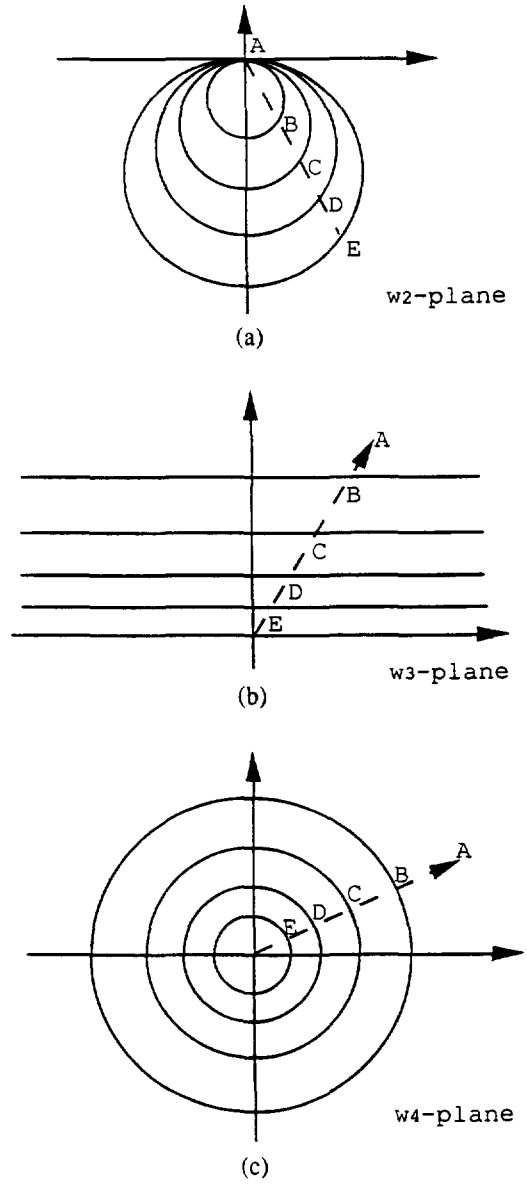

Fig. A.2. Configurations at different transformation stages.

This mapping is a translation of $\sigma_0+i\tau_0$, as defined in Fig. A.1(a), so that the unloading point A gets mapped to the origin in the w_1 plane.

$$w_2 = w_1 e^{i[(\pi/2)-\theta_0]}: \quad (w_2 \equiv \sigma_2 + i\tau_2 \equiv r_2 e^{i\theta_2}) \tag{II}$$

The second mapping is a counterclockwise rotation of $\pi/2-\theta_0$, where θ_0 is defined in Fig. A.1(a). After the two transformations w_1, w_2, the geometrical configuration in the z plane (Fig. A.1(a)) is mapped onto that in the w_2 plane, as shown in Fig. A.2(a).

$$w_3 = \frac{2}{w_2}: \quad (w_3 \equiv \sigma_3 + i\tau_3 \equiv r_3 e^{i\theta_3}) \tag{III}$$

This mapping maps the circles in the w_2 plane into horizontal lines in the w_3 plane, as shown in Fig. A.2(b).

$$w_4 = (r_3 \sin\theta_3) e^{i(2\theta_3-\theta_0)}: \quad (w_4 \equiv \sigma_4 + i\tau_4 \equiv r_4 e^{i\theta_4}) \tag{IV}$$

This mapping maps the horizontal lines in the w_3 plane into concentric circles in the w_4 plane, as shown in Fig. A.2(c). It has also been chosen so that the direction of a plastic strain increment, which is determined using the normality principle, is preserved after transformation. To make the idea clearer, let us look at the two plots

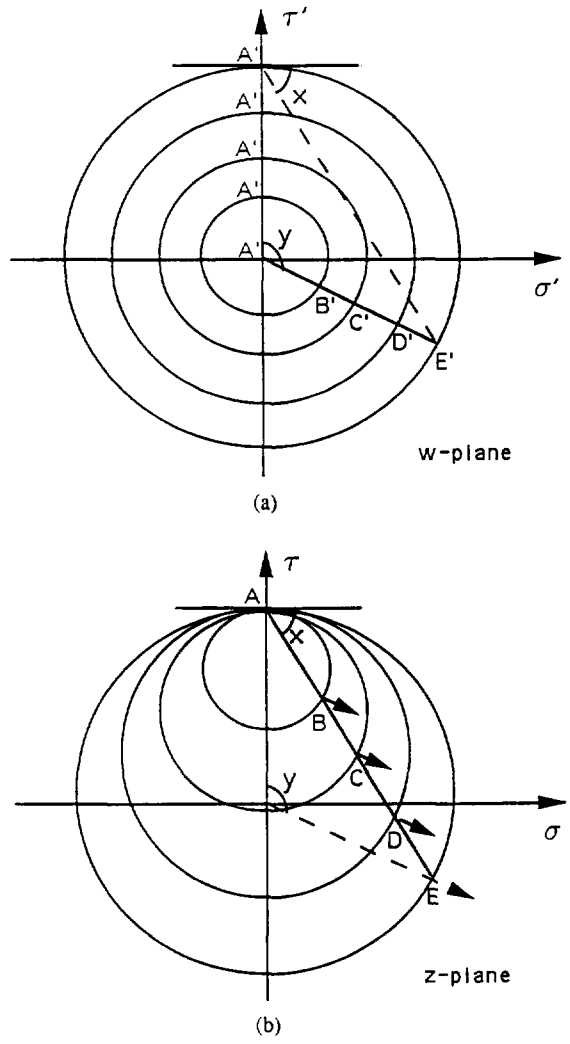

Fig. A.3. Conditions of the principle of normality on the proposed transformation.

in Fig. A.3(a) and (b), which show respectively, the geometrical configurations after and before transformation for the special case $\theta_0 = \pi/2$. In order to meet the normality rule, we need that the points A, B, C, and D in Fig. A.3(b) be mapped to A', B', C', and D' in Fig. A.3(a) so that they have exactly the same outward normal direction. Thus, by geometry we require that

$$\angle x = \tfrac{1}{2}\angle y, \quad \angle y = \theta_0 - \theta \tag{A1}$$

where θ is the angle that the outward normals shown in Fig. A.3(b) make with the σ-axis. It can be easily shown that the transformation formula w_4 given in (IV) satisfies the conditions required by (A1).

$$w = \frac{1}{w_4}: \quad (w \equiv \sigma' + i\tau') \tag{V}$$

The geometrical configuration after this transformation can be found to be just the one shown in Fig. A.1(b), in which the coordinates of the unloading point A' is the same as those of point A in Fig. A.1(a).

Based on the above, the overall transformation which maps the configuration in Fig. A.1(a) to that in Fig. A.1(b) can be found to be

$$w = \frac{r_1}{2\sin\theta_2} e^{-i\theta_4}$$

where

$$r_1 = \sqrt{(\sigma-\sigma_0)^2+(\tau-\tau_0)^2}$$

$$\theta_1 = \tan^{-1}\left(\frac{\tau-\tau_0}{\sigma-\sigma_0}\right), \quad \theta_0 = \tan^{-1}\left(\frac{\tau_0}{\sigma_0}\right)$$

$$\theta_2 = \theta_1-\theta_0+\frac{\pi}{2}, \quad \theta_4 = \pi-2\theta_1+\theta_0$$

Equations (13) and (14) are simply these equations together with the appropriate transformation to ensure that the Von Mises or Tresca yield function gives circles for the yield surfaces in 2-D space.